Realistic Independent-Particle Model of the Nucleus*

ALEX E. S. GREEN
Department of Physics, The Florida State University, Tallahassee, Florida
(Received November 7, 1955)

A phenomenological central potential is explored which is characterized by a universal depth (V_0), a universal surface extension (d), and an inner radius function $a=a_1A^{\frac{1}{3}}+a_0$. The four parameters are adjusted to be in accord with experimental information obtained from low-energy neutron scattering and from neutron separation energies. The results $V_0=40$ Mev, $d=1$, $a_1=1.32$, and $a_0=-0.8$ (all in units of 10^{-13} cm), are in reasonable accord with what might be expected from other experimental and theoretical considerations. Since the experimental data used in the adjustment process bound the energy region in which the discreteness of nuclear energies is most evident, one might expect that the eigenvalues and eigenfunctions based upon this phenomenological model would furnish a highly realistic set for the theoretical study of low-energy nuclear transitions within the framework of the independent-particle model of the nucleus.

The energy eigenvalues and the important parameters for the energy eigenfunctions are calculated by a procedure suitable for the restricted type of potential under consideration. A simple method is presented for handling small perturbations, particularly the Coulomb perturbation. In the latter case, it is shown that the derived proton eigenvalues agree with experimental proton separation energies, provided one introduces an anomalous attractive potential which cancels approximately one-half of the classical Coulomb potential acting upon an individual proton. The implications of these results are discussed.

(1) SIMPLE NUCLEAR MODEL

A PREVIOUS study[1] has shown that it is possible to locate the $3s$ and $4s$ maxima in the theoretical neutron cross-section surface at prescribed A values and at the same time to match the general trends of neutron binding energies by interpolating between exponentially diffuse potential wells with appropriate degrees of diffuseness. If, as current studies of neutron scattering indicate,[2,3] these A values are near 55 and 170, respectively, then the required diffuseness parameter δ, which is defined as the tail length to the $1/e$ point divided by the radius of the uniform region, drifts from about 0.3 for light nuclei to about 0.13 for heavy nuclei. The fact that this ratio falls off quite substantially led to the investigation of a simple model which embodies such a decrease. The model chosen has an inner region of constant depth V_0 whose radius is given by

$$a=a_1A^{\frac{1}{3}}+a_0, \tag{1}$$

and an outer exponentially decreasing region with the decay length d to the $1/e$ point. V_0 and d are the same for all nuclei. The procedure used in fixing the four constants V_0, d, a_1, and a_0 was as follows: First a set of theoretical neutron binding energies for $\delta=d/a=0$, 0.1, 0.2, 0.3 and 0.4 were prepared using the eigenvalues of GL1.[4] These were similar to Fig. 2 of reference 1, but with 55 and 170 taken as the locations for the $3s$ and $4s$ neutron cross section maxima instead of 55 and 150. Using the empirical neutron binding energy line corresponding to $V_0\sim40$ Mev, the δ's needed to produce approximate agreement were then determined by interpolation for 10 equally spaced values of A. Ignoring the small reduced-mass effect, one may define a well parameter

$$\epsilon_0=(2mV_0/\hbar^2)^{\frac{1}{2}}a=(V_0/U_0)^{\frac{1}{2}}a, \tag{2}$$

where $U_0=20.734$ Mev and a is in units of 10^{-13} cm. The assumption of a constant diffuseness distance implies

$$\delta=da^{-1}=C\epsilon_0^{-1}. \tag{3}$$

Using $f_1(\delta)$ and $f_2(\delta)$ functions determined to secure the critical $3s$ and $4s$ A values of 55 and 170, and inserting the 10 interpolated δ's into

$$\epsilon_0=f_1(\delta)A^{\frac{1}{3}}+f_2(\delta)=C\delta^{-1}, \tag{4}$$

the values of C were obtained for each of the ten A's. These were found to be approximately compatible with $C=1.389$. Since ϵ_0 and δ are now rigidly tied together, ϵ_0 is now a function of A alone. Replacing the δ in Eq. (4) by $C\epsilon_0^{-1}$ and solving for ϵ_0 *vs* A, it was found that the function so obtained could be fitted quite accurately by the equation

$$\epsilon_0=1.833A^{\frac{1}{3}}-1.111. \tag{5}$$

The constant V_0 was next fixed by insisting that the general trends of the predicted particle binding energies match the experimental trend. This led to $V_0=40$ Mev,

$$d=C(U_0/V_0)^{\frac{1}{2}}=1, \tag{6}$$

and

$$a=\epsilon_0C^{-1}=1.32A^{\frac{1}{3}}-0.8, \tag{7}$$

where all distances are in units of 10^{-13} cm. It is important to note that while a change in V_0 will produce a proportionate change in the energy eigenvalues, it will have a lesser effect upon the corresponding diffuseness distance and radius function. Accordingly, a modest

* This investigation was supported by a grant from the U. S. Atomic Energy Commission.
[1] A. E. S. Green, Phys. Rev. **99**, 1410 (1955).
[2] W. S. Emmerich, Phys. Rev. **98**, 148(A) (1955) and private communication.
[3] Weisskopf, Porter, and Feshbach, Proceedings of the International Conference on the Peaceful Uses of Atomic Energy 8/P/830, 1955 (to be published).
[4] A. E. S. Green and K. Lee, Phys. Rev. **99**, 772 (1955). This work will henceforth be referred to as GL1. The analysis and notation in GL1 are applicable here unless otherwise noted.

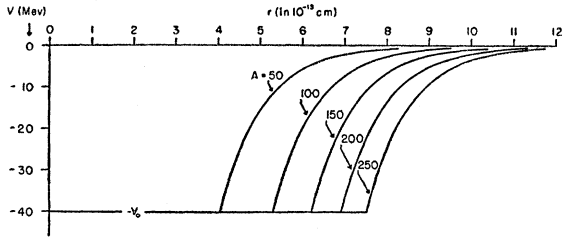

FIG. 1. The nuclear potential for several representative values of A.

change in V_0 might well be used to make a final improvement in predicted particle energies.

The above rather roundabout procedure is essentially a method of determining the four parameters V_0, d, a_0, and a_1 in terms of four experimental data, i.e., the critical $3s$ and $4s$ A values and the slope and constant in the linear function which characterizes the general trends of neutron binding energies. It is rather satisfactory to note that the radius function, well depth, and diffuse distance so derived are in reasonable accord with those which have been obtained from a great variety of other experimental data. The model arrived at here is illustrated in Fig. 1.

The functions $a(A)$, $\delta(A)$, and $\epsilon_0(A)$ characterizing this model are presented in Fig. 2 along with the parameter α^2 which, in conjunction with the equation

$$r^{-2}\approx a^{-2}\{\alpha^2+(1-\alpha^2)\exp[-(r-a)/d]\}, \qquad (8)$$

approximately characterizes the centrifugal energy in the outer region.

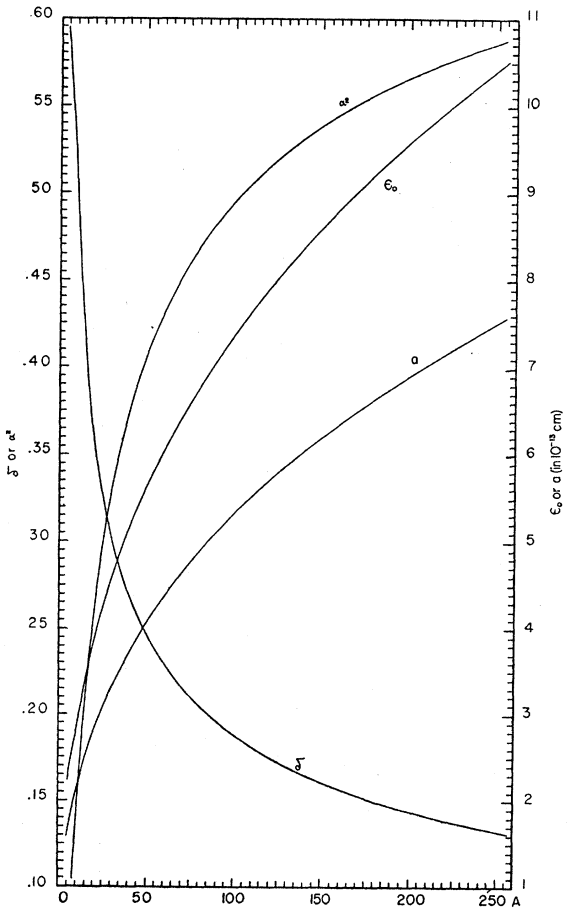

FIG. 2. The well parameters a, δ, and ϵ_0 and the centrifugal energy parameter α^2, all as functions of A.

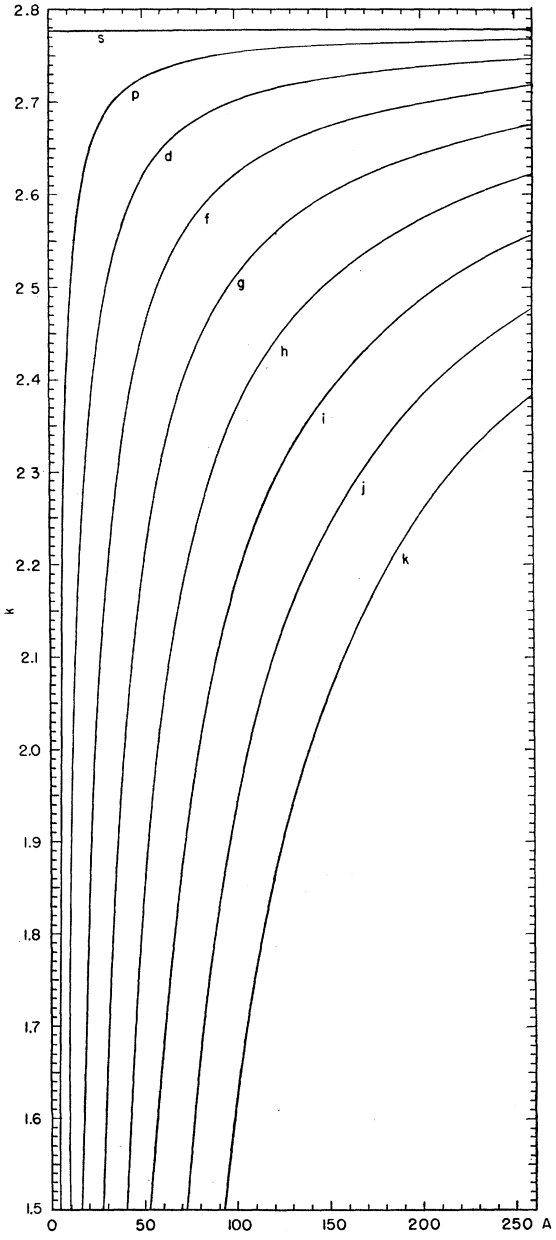

FIG. 3. The wave-function parameter k as functions of A for various states of orbital angular momentum.

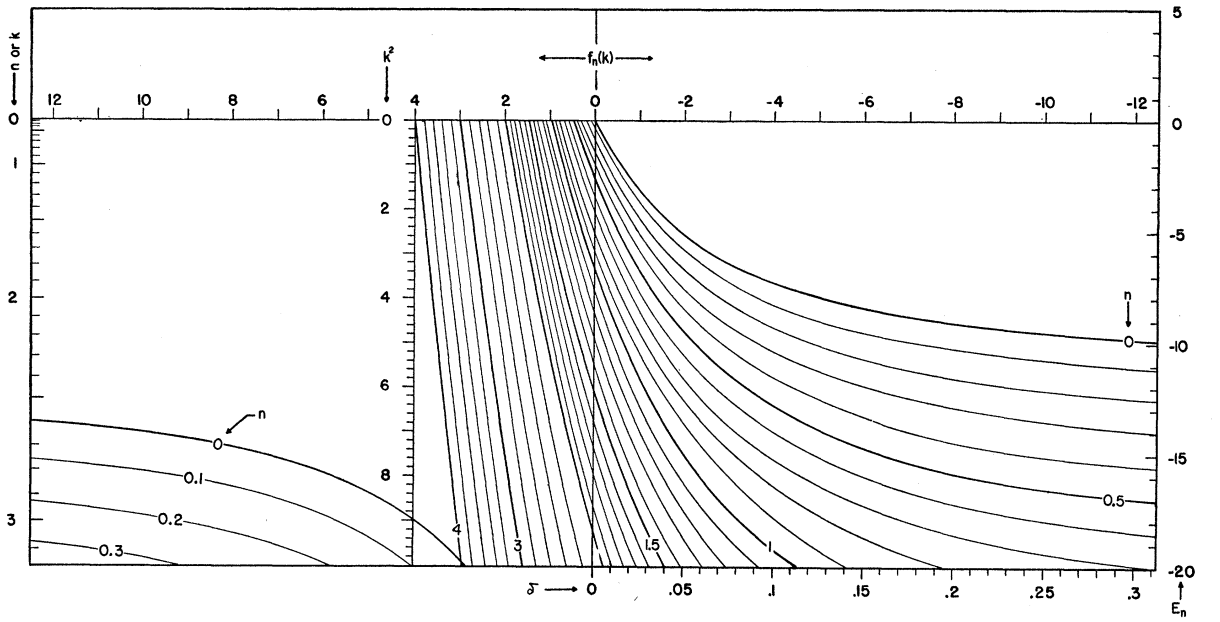

FIG. 4. Nomogram for obtaining the logarithmic derivative of the exterior wave function. First select the ordinate corresponding to k^2 and the abscissa found by interpolating between n-contours. Transfer this point vertically to a line joining the zero index and the value of δ at the lower right scale, and then carry it horizontally to the right scale. The result corresponds to the value of $E_n(k,\delta)$.

(2) DETERMINATION OF THE EIGENVALUES

Since the particular family of potentials arrived at in the previous section are contained in the work of Green and Lee,[4] the analysis and results of this earlier investigation are applicable here. In particular, approximate eigenvalues may be obtained by interpolating between their eigenvalue curves for $\delta=0$, 0.1, 0.2, 0.3, and 0.4. A preliminary study by this method indicated that some of the key parameters intrinsic to the specific model now under study are far more restricted than those considered in GL1. Accordingly, in the interests of achieving the greatest accuracy within these restricted ranges, it appeared best to develop a direct method for determining the eigenvalues. The technique developed here may also be of interest in connection with other types of compound potentials.

The important outer wave-function parameter k, which is given in this special model by

$$k=[7.717-4\delta^2(1-\alpha^2)l(l+1)]^{\frac{1}{2}}, \tag{9}$$

is presented in Fig. 3.

According to Eqs. (21) and (22) of GL1, the negative of the logarithmic derivative of the external wave function is a three-parameter function given by

$$E_n(k,\delta)=\{n-k[J_{n+1}(k)/J_n(k)]\}(2\delta)^{-1}. \tag{10}$$

In GL1 a transformation made it possible to obtain values of $E_n(k,\delta)$ from the graph of $I_l(\epsilon')$, the negative of the logarithmic derivative of the internal wave function. This transformation is not useful here because of the restricted range of the diffuseness parameters. Therefore, it was imperative in this study to develop tables and graphs for obtaining the logarithmic derivative of the external wave function for fine intervals of n and k within the restricted range of from 0–3. Using all available tables of fractional Bessel functions and evaluating various special cases by series and recurrence relationships, the function

$$f_n(k)=n-k[J_{n+1}(k)/J_n(k)] \tag{11}$$

was generated. The values of this function so obtained are presented in Fig. 4. Here the horizontal scale represents $f_n(k)$ for the values of n which label the curves and for the vertical coordinates which correspond to the k^2 values. To obtain the actual logarithmic derivatives for various δ, a scale for graphical division by 2δ is provided on the lower right. The scales are chosen so that the output $E_n(k,\delta)$ on the right is on the same scale as that used for $I_l(\epsilon')$ in GL1, Fig. 1. Thus by coupling the two graphs, the process of matching the logarithmic derivatives can be accomplished mechanically.

The scale to the extreme left on Fig. 4 represents values of n and, in conjunction with auxiliary scales, provides a method which automatically accomplishes the solution of

$$k^2-n^2=4\delta^2[\epsilon'^2-l(l+1)]. \tag{12}$$

A typical set of auxiliary scales which automatically introduce the factor $4\delta^2$ is shown in Fig. 5. The lines labeled by letters are positioned at the values of $l(l+1)$. The appropriate foreshortenings were determined by swinging an arc of length $k^2=7.717$ on the scale of Fig. 4 and drawing radial lines such that the intersections on

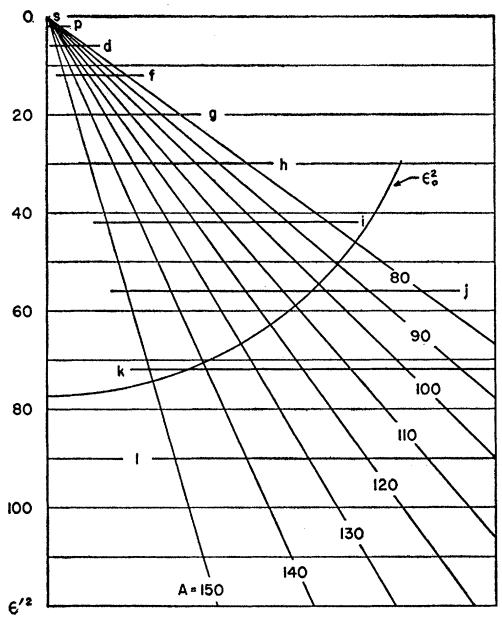

FIG. 5. Auxiliary scales. To solve Eq. (10), align the line corresponding to the value of A with the left vertical scale of Fig. 4. Setting the l index at the value of n, one reads the value of ϵ'^2 next to the value of k.

the scale of Fig. 5 correspond to the value of ϵ_0^2 for each A. It follows from Eq. (17) of GL1 that for $l=0$, this procedure gives a compressed scale which multiplies any distance on the scales in Fig. 5 by the factor $4\delta^2$ when that distance is read on the k^2 scale of Fig. 4.

The procedure for finding the n and ϵ' eigenvalues once k, l, and δ are prescribed is as follows: (a) Place a thin horizontal straight edge at the value of k^2. (b) Set the auxiliary scale such that the l index corresponds to an initially assumed value of n. (c) Read the corresponding value of ϵ'^2 on the auxiliary scale. (d) Going to the ϵ'^2 on Fig. 1 of GL1 obtain the value of $I_l(\epsilon')$. (e) Transfer horizontally through the right scale of Fig. 4 to the 2δ dividing line, and then transfer vertically to the horizontal level corresponding to k^2. If the corresponding value of n interpolated from the family of curves does not agree with the initially assumed value, a new n is chosen and the cycle repeated. This rapidly convergent process is continued until agreement is achieved. One thus obtains the n and ϵ' eigenvalues which are simultaneous solutions of $E_n(k,\delta)=I_l(\epsilon')$ and Eq. (12). These results are shown for the complete range of A in Figs. 6 and 7. Considerable care and effort were expended towards eliminating error in these graphical determinations. In general, the work was repeated where necessary until significant incon-

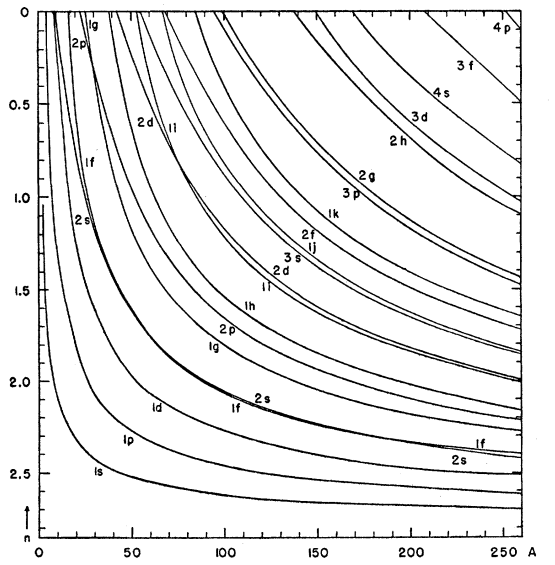

FIG. 6. Wave-function parameter n as a function of A for various states.

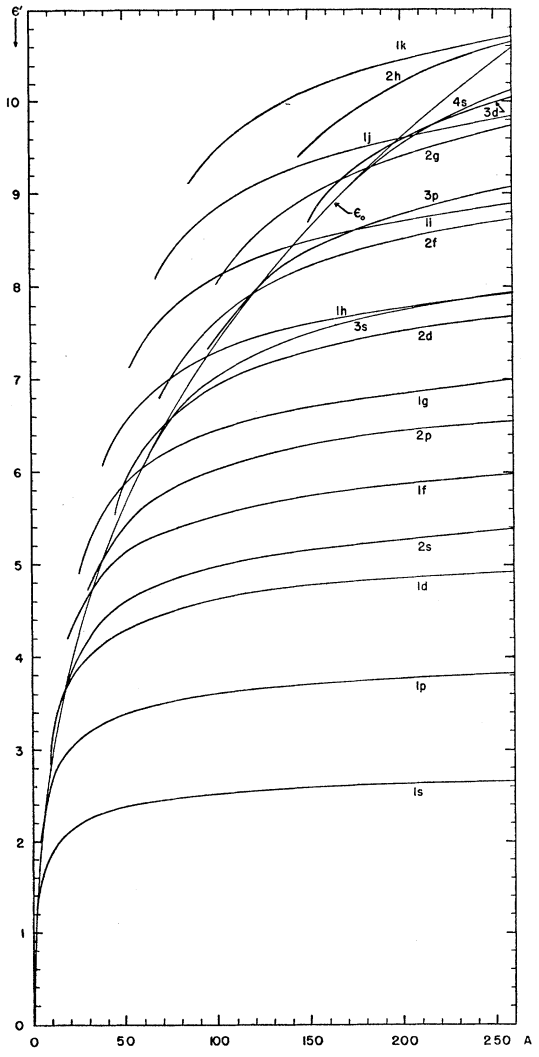

FIG. 7. Wave-function parameter ϵ' as a function of A for various states. The portions of the curves to the left of the ϵ_0 curve correspond to positive energy states.

sistencies were eliminated. It is estimated that the precision of these determinations was such that the probable error would not exceed two line widths.

It is interesting to observe in Fig. 7 that, for other than s states, discrete positive energy eigenvalues are obtained. These correspond to states virtually bound by the centrifugal barrier. This method of approximation which neglects leakage becomes somewhat suspect for the states of higher l close to the top of the centrifugal barrier. However, one may be fairly confident of those just above zero and of the eigenvalues for low l values.

The absolute energy eigenvalues are shown in Fig. 8 based upon the choice $V_0=40$. The fact that the $3s$ and $4s$ levels intersect $W=0$ near 55 and 170 confirms the efficacy of a part of our involved adjustment process.

The locations of the outermost neutrons for beta-stable nuclei with 10, 20, 30, $\cdots$ neutrons are indicated by square symbols in Fig. 9. The line labeled $B_n{}^e$ represent the general trends of experiment [see Eq. (12), reference 1]. It will be noted that these are in general agreement which further illustrates the efficacy of this well parameter adjustment process. It should be remarked that the inclusion of spin-orbit splittings will not only reduce the sizes of the discontinuities and generate the well-known magic numbers, but it will also depress slightly the general trends of the predicted energies. The splittings, of course, directly lower the states for $i=l+\frac{1}{2}$. While the states for $i'=l-\frac{1}{2}$ are raised, nevertheless, since these states fill up at slightly larger A values, a small systematic downward shift results. For reasonable spin-orbit splittings, this effect helps to improve further the agreement between the predicted and the empirical neutron energies. Before considering the proton energies shown in Fig. 9, it is necessary to develop a method for handling perturbations.

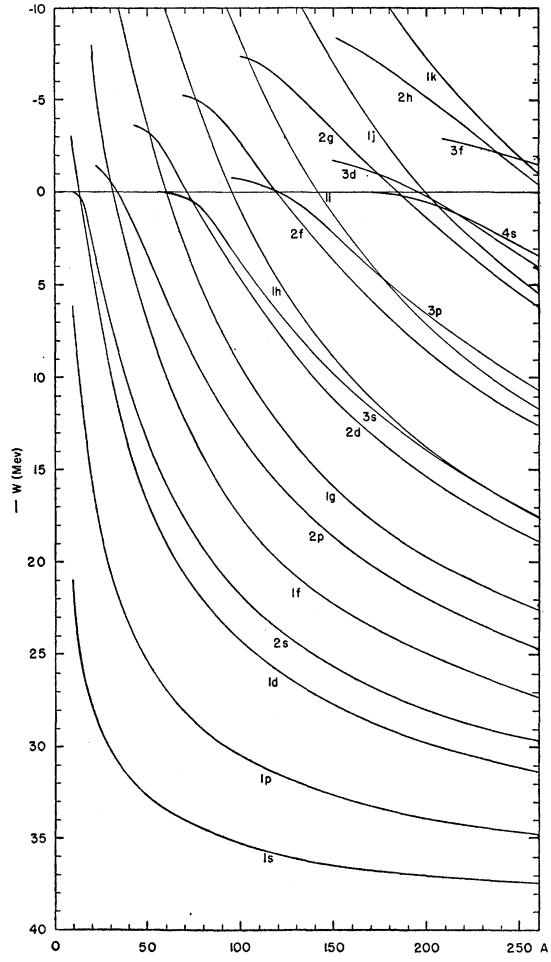

FIG. 8. Neutron energy eigenvalues for various values of A.

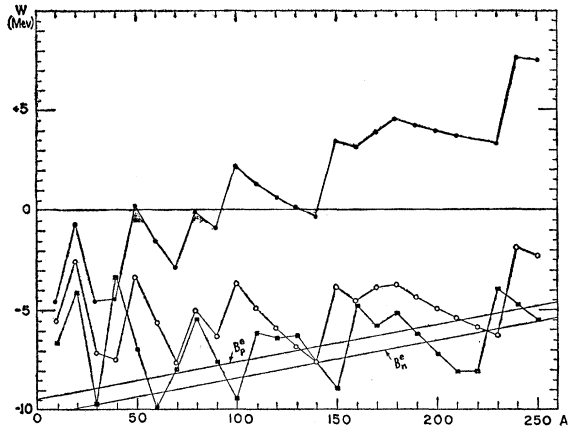

FIG. 9. The energies of the outermost protons and neutrons in beta-stable nuclei. The open circles denote values computed with one-half the classical Coulomb potential. The closed circles denote values computed with the full classical Coulomb potential. The squares denote neutron energies. The straight lines represent the empirical energies.

(3) PERTURBATION METHOD

It is desirable to extend the usefulness of the eigenvalues and the eigenfunctions corresponding to this simple nuclear model so that they may be applied to closely comparable potential forms. A simple and direct basis for doing so employs the fact that the parameters which characterize a square well enter the dimensionless radial wave equation only through the dimensionless well strength parameter

$$\epsilon_0{}^2=V_0(2ma^2/\hbar^2). \tag{13}$$

Since nuclear potentials fall off rather sharply, one might, as a first step, seek a procedure for finding the equivalent square well strength of an arbitrary well with a diffuse boundary. An obvious parameter for an arbitrary well which goes over to $\epsilon_0{}^2$ for the square

well is

$$S=2(2m/\hbar^2)\int^{\infty} V(r)rdr. \tag{14}$$

On this basis, the equivalent well strength of the model under study here is

$$S=\epsilon_0^2(1+2\delta+2\delta^2)=\epsilon_0^2+2C\epsilon_0+2C^2. \tag{15}$$

It might be noted that for small δ this result corresponds approximately to an earlier definition for equivalence derived from the locations of the $2s$, $3s$, and $4s$ wave maxima [see Eq. (16), reference 1]. The function S for various values of A in our simple nuclear model is plotted in Fig. 10. Using Eq. (12) to compute S, this curve may be used to find the equivalent A corresponding to an arbitrary nuclear potential. To apply this method to small perturbations in such a manner as to minimize the uncertainties in the definition of equivalent square well strength, one may calculate the shift in A by means of

$$\Delta A=(dA/dS)\Delta S=[0.5890A^{\frac{1}{3}}/(a+1)]\Delta S. \tag{16}$$

The coefficient of ΔS is also plotted in Fig. 10.

When the perturbing potential is proportional to $V(r)$, i.e., $v=kV(r)$, the shift in A is given by $\Delta A=kS(dA/dS)$. $S(dA/dS)$ is also plotted on Fig. 10.

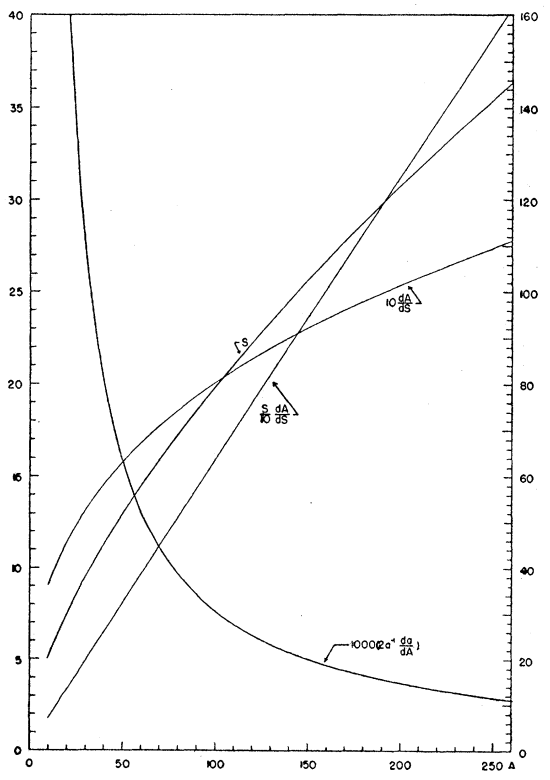

FIG. 10. Functions for calculating equivalent A. S is to be read on the right scale.

Having obtained an equivalent A, the task still remains of finding the appropriate radius parameter In the latter case, of course, the unperturbed radius parameter is to be used. However, for other perturbations or other potentials, some alteration of a may be essential.

The following procedure is regarded as a reasonable one for a monotonically decreasing potential $V(r)$. One first calculates r_1, r_2, and r_3 which satisfy

$$V(r_1)=0.9V(0),\ V(r_2)=0.5V(0),\ V(r_3)=0.1V(0). \tag{17}$$

Using the characteristics of our simple exponential model, the effective d may then be determined by letting

$$r_3-r_1=2.197d. \tag{18}$$

The effective a then follows from

$$a=r_2-0.6932d. \tag{19}$$

Alternatively, one might use a variety of graphical procedures for finding a suitable a to be associated with the equivalent A. The ultimate objective in these procedures is to find the member of the set of dimensionless potentials, characterized in our model by A alone, which most nearly corresponds to a dimensionless form of the exact potential. If the residual between the dimensionless exact potential and the dimensionless model potential undergoes several alternations in sign, then, not only will the error in the energy eigenvalue be small, but, apart from small local differences, the model wave function for the equivalent A will be close to the exact wave functions. The second-order effect of the residual (including the residual centrifugal energy) upon the eigenvalues and eigenfunctions can finally be determined by numerical methods.

(4) COULOMB CORRECTION FOR PROTONS

If one assumes that each proton experiences the Coulomb repulsion of the remaining protons as well as the nuclear potential, one must use a modified potential well for protons. To arrive at the effective individual particle potential for each proton, one must first make a reasonable assumption as to the proton distribution. Thus, one must, in effect, solve the complete self-consistent field problem for the nucleus. Since, however, the Coulomb potential energy is a relatively small perturbation and rather insensitive to the fine details of the charge distribution, it is possible to proceed on the basis of almost any reasonable distribution of protons in arriving at an appropriate potential energy for a single proton. The procedure followed here shall be based on the assumption that the $Z-1$ protons which act upon the last proton are distributed according to

$$\begin{aligned}\rho(r)&=\rho_0, && r<a_c,\\ &=\rho_0\exp[-(r-a_c)/d], && r>a_c,\end{aligned} \tag{20}$$

where ρ_0 is a constant and a_c and d_c are lengths which characterize the charge distribution. On the basis of a classical calculation, the Coulomb potential of a single proton is

$$V_c(r)=\frac{(Z-1)e^2}{a_c\lambda_c}\left[\mu_c-\frac{r^2}{6a_c^2}\right], \quad r<a,$$
$$=\frac{(Z-1)e^2}{r}\left[1-\frac{\delta_c^2}{\lambda_c a_c}(r+2\delta_c a_c)\exp\left(\frac{a_c-r}{d_c}\right)\right], \quad r>a, \quad (21)$$

where

$$\mu_c=\tfrac{1}{2}+\delta_c+\delta_c^2 \quad (22)$$

and

$$\lambda_c=\tfrac{1}{3}+\delta_c+2\delta_c^2+2\delta_c^3. \quad (23)$$

In seeking an equivalent A which will correct for the major effect of the Coulomb perturbation, one is immediately confronted with the fact that the ΔS for the Coulomb perturbation diverges. However, the slow decay of the Coulomb perturbation suggests an approximation in which Coulomb potential energy is replaced by a constant plus an additional potential which is proportional to the nuclear potential [see Eq. (11) and Table II, reference 1]. The constant term simply causes a corresponding shift in the proton energy without altering the wave function. The term proportional to the nuclear potential, however, not only effects the energy, but also influences the wave functions. The major corrections to the energy as well as to the wave functions may be determined by the perturbation method discussed in the previous section. The shift in A is simply given by

$$\Delta A=-(Z-1)[2\alpha(\delta)U_c/V_0a]S(dA/dS), \quad (24)$$

where α is the function given in Table III of reference 2 and $U_c=0.8639$ Mev.

In using the eigenvalues given in Fig. 8 for the equivalent A, one must take note of the fact that these eigenvalues represent $W=\epsilon_w^2(\hbar^2/2ma^2)$. Thus the desired proton eigenvalues which include the effect of the constant term are given by

$$W=W(A')(a'^2/a^2)+2(Z-1)U_c\beta/a,$$
$$\approx W(A+\Delta A)[1+2a^{-1}(da/dA)\Delta A]+2(Z-1)U_c\beta/a, \quad (25)$$

where β is the second function in Table III of reference 2. The function $2a^{-1}(da/dA)$ is also shown in Fig. 10.

Using Eq. (24), the proton binding energies have been calculated for beta-stable nuclei with $Z=10$, 20, etc. These are indicated by the solid circles in Fig. 9. The experimental trend is indicated in this figure by the line labeled $B_p{}^e$. It should be clear that the proton binding energies obtained by adding the classical Coulomb potential energy are highly unsatisfactory. Indeed this calculation indicates that the last proton in medium and heavy nuclei is not even bound. One obtains fairly satisfactory proton binding energies if one adds only one-half the Coulomb potential energy to the nuclear potential. The results based upon such a perturbation are indicated by the open circles in Fig. 9. The efficacy of the use of one-half the Coulomb potential to provide satisfactory proton binding energies has been checked by more direct perturbation methods and seems strongly established.

It is tempting to relate this empirically established factor of one-half with the two-body character of the electrostatic interaction in the sense that only one-half of the Coulomb interaction energy of a single proton with the remaining protons may be taken as the "share" of this proton. The independent-particle-model Coulomb perturbation was used in reference 2 as well as the one chosen in a recent work by Bleuler and Terreaux.[5] This explanation might be objected to on the grounds that the Hartree self-consistent field method for many-electron systems, which requires corrections for the two-body effect in total energy calculations, nevertheless, leads to separation energies which are approximately equal to the eigenvalues computed on the basis of the full Coulomb potential energy.[6] One might, of course, question whether these results are applicable to the nucleus—a system so vastly different from the atom in its density and compressibility. It should be clear that an equivalent device to reduce the Coulomb potential energy by one-half would be to assume that in addition to the neutron potential and the full classical Coulomb potential each proton feels an anomalous attractive potential which cancels approximately one-half the repulsive Coulomb potential. In the absence of an understanding as to the origin of the shell model potential, this interpretation should be relatively free from objection at this time. An important argument in favor of the idea of an attractive proton anomaly has come out of a recent analysis of low-energy proton scattering.[7] To facilitate a quantitative study of the proton potential, the total proton perturbation will be represented by

$$v_p=v_c+v_a, \quad (26)$$

where v_c is the full classical Coulomb perturbation and v_a is the additional anomaly. Let it be assumed that the proton density distribution is characterized by Eq. (20), and consequently the classical Coulomb potential acting on an individual proton is given by Eq. (21). Since the inner radius function $a=1.32A^{\frac{1}{3}}-0.8\approx 1.16A^{\frac{1}{3}}$ is slightly smaller than the radii of the nuclear charge distribution as observed in electron scattering and μ-mesonic x-ray studies, it is not unreasonable for initial studies to let $a_c\approx a$, provided one uses a proton decay length which is smaller than the decay length

[5] K. Bleuler and Ch. Terreaux, Helv. Phys. Acta **28**, 254 (1955).
[6] E. V. Condon and G. H. Shortley, *The Theory of Atomic Spectra* (Cambridge University Press, Cambridge, 1955).
[7] Melkanoff, Moskowski, Nodvik, and Saxon, Phys. Rev. **101**, 507 (1956).

of the nuclear potential. The effect of the classical perturbation acting upon the proton may now be treated by the perturbation methods developed in the preceding section. A simpler and more direct way will now be used for computing the well-strength change associated with the slowly decreasing Coulomb potential. This method involves introducing a cut-off radius r_c beyond which the classical Coulomb perturbation has no appreciable effect upon bound states. If r_c is expressed in the form $a+nd_c$, where n is a pure number, the Coulomb energy at this distance is

$$v_c(r_c)=(Z-1)e^2(a+nd_c)^{-1}\times\{1-\delta_c^2\lambda^{-1}[1+(n+2)\delta_c]e^{-n}\}. \quad (27)$$

Assuming that $nd_c\approx d$, which is essentially choosing the cutoff at $a+d$, and then estimating n to be of the order of 2–5, it clearly becomes safe to ignore the second term in the bracket. Accordingly, one may make a partial correction for the effect of the classical Coulomb perturbation upon bound states of protons simply by raising the proton energy levels by

$$v_c(r_c)=(Z-1)e^2/(a+d). \quad (28)$$

A comparison of this with the classical expression $6(Z-1)e^2/5R$, based upon the assumption that the outermost proton and the remaining protons are uniformly distributed over the radius R, suggests that Eq. (28) accounts for the bulk of the classical Coulomb effect. To correct for the small residual influences on both the wave functions and the eigenvalues, the approximate method outlined in Sec. 3 may be used. According to this procedure, this residual Coulomb perturbation causes a well-strength change

$$\Delta S_c=-2\left(\frac{2m}{\hbar^2}\right)\int_0^{r_c}[v_c(r)-v_c(r_c)]rdr$$
$$=(2ma^2/\hbar^2)(Z-1)e^2(12\lambda_c a)^{-1}\{1+12\lambda_c\delta_c n-12\delta_c^2-48\delta_c^3-48\delta_c^4+12\delta_c^2e^{-n}\times[1+(2n+4)\delta_c+(2n+2)^2\delta_c^2]\}. \quad (29)$$

Expanding λ_c and ignoring terms of the order of δ_c^2 and higher, it follows that the A shifts associated with the residual Coulomb perturbation are given by

$$\Delta A_c=-(dA/dS)\epsilon_0^2(Z-1)(5U_c/12V_0a)\times[1+4n\delta_c-3\delta_c]. \quad (30)$$

For the purposes here, it is sufficiently accurate to let $n\delta_c=\delta$ in the second term in the bracket and $3\delta_c\approx\delta$ in the third term. The Coulomb A shifts so computed are given in Table I.

In view of the previously noted success from the particle binding energy standpoint of the simple device of reducing the Coulomb interaction by one-half, one is led to investigate the possibility that the anomaly is indeed associated with a direct distortion of the Coulomb interaction. For greater realism, it shall be assumed here that the distortion occurs only on the inside of the nucleus. As a simple exploratory step, borrowing from well-known atomic methods, let it be assumed that the proton anomaly is the product of the Coulomb interaction and a dimensionless function $\varphi(r)$ which is close to zero at r_c and which builds up rapidly to $-k$ as one proceeds towards $r=0$. If for simplicity this function is taken as

$$\varphi(r)=-k,\ r<a;\ \varphi(r)=-k\exp[(a-r)/d_a],\ r>a, \quad (31)$$

it follows by calculations analogous to those leading to Eq. (29) that the A shift due to the anomaly (to linear order in δ_c but exact in $\delta_a=d_a/a$) is

$$\Delta A_a=25k(Z-1)\epsilon_0^2(12a)^{-1}\{1-(3/5)\delta_c+(8/5)\delta_a[1-\exp(-d/d_a)]\}dA/dS. \quad (32)$$

If as previously assumed $\delta_c\ll\delta$, the second term can safely be ignored, and if $\delta_a\sim\delta$ the third term makes only a small contribution. For concreteness and to conform to the assumption that $\varphi(r)$ is small near $r_c=a+d$, it shall be assumed that $d_a=\frac{1}{2}d$. The A shift due to this anomaly as well as the net A shift then may be computed for any choice of k. The final expected proton energies are given by Eq. (25) but with $v_c(r_c)$ replacing the second term and with ΔA representing the net A shift. After investigation of the consequences of a number of choices of k, the value $k=0.7$ was found to yield proton binding energies in approximate accord with the experimental trends. The A shifts associated with this anomaly and the net A shifts are also given in Table I. Particle binding energies based upon these

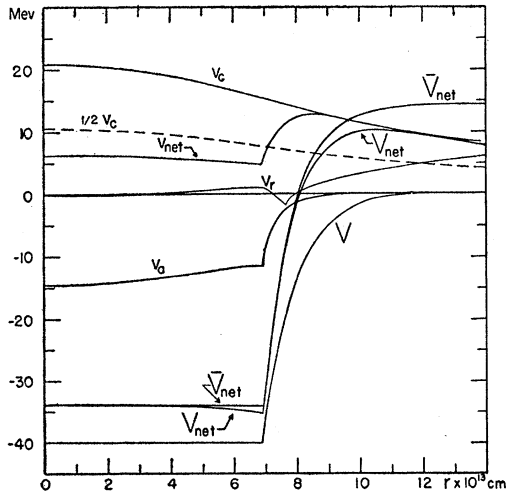

FIG. 11. Illustration of the general nature of the potentials assumed to act in a heavy nucleus ($_{80}Hg^{200}$). V denotes the nuclear potential, v_c the Coulomb potential, v_a the anomaly based upon Eqs. (31) and (20) with $k=0.7$, and v_{net} the net perturbation. V_{net} is the net potential acting upon a proton, $\bar{V}_{\text{net}}$ is the approximate one used in this analysis, and v_r is the residual which is ignored.

ΔA's conform quite closely to the $B_p{}^e$ line in Fig. 9. An illustration of the general nature of the potentials which are assumed to act in a typical heavy nucleus ($_{80}Hg^{200}$) is shown in Fig. 11. V here denotes the nuclear potential, v_c the Coulomb potential, v_a the anomaly based upon Eqs. (31) and (20) with $k=0.7$. v_{net} is the net perturbation acting upon a proton. Also shown on this diagram is $\frac{1}{2}v_c$, which clearly provides a moderately good average representation of the net perturbation. The net potential acting upon a proton is indicated by V_{net}. The approximate proton potential used in this analysis which is arrived at by the cut-off device and the method of A shifts is denoted by $\bar{V}_{\text{net}}$. The residual, $v_r=V_{\text{net}}-\bar{V}_{\text{net}}$, which is ignored in this analysis, is also shown. It is satisfactory that even in the case of a heavy nucleus this residual is small in the region of importance and changes sign several times. The effect of the residual which varies somewhat from state to state, could be handled in the next approximation by numerical methods.

The overall agreement between $\frac{1}{2}v_c$ and v_{net} indicates that both devices would be about equally effective from the standpoint of particle binding energies. The differences between these two perturbations would, however, influence the wave functions. Because of the slow decline of v_c, this perturbation would push out the proton probability distribution relative to the neutron distribution in the same quantum state. On the other hand the abrupt rise in v_{net} indicates that with the alternative interpretation the proton is pulled in relative to a neutron in the same quantum state. The extent of these effects will be examined in a later paper in which the wave functions will be developed.

(5) DISCUSSION AND CONCLUSIONS

It might be hoped that the reasonableness and success of this simple model might shed some light on the relationship between the theory of nuclear forces and the phenomenological nuclear potentials required for shell model studies. The proton potential anomaly must certainly be a significant clue in this direction. While the potential anomaly described here has been related to the Coulomb effect, it is important to point out that alternative interpretations concerning the origin of the anomaly have been examined which also yield satisfactory proton binding energies. These will be reported in a later work. For the moment, it is perhaps best to use the net A shifts and the constants given in Table I to characterize the net perturbing force acting upon protons without regard to their interpretation.

The fact that in this model the region of buildup of the nuclear potential occurs in a distance of the order of 1×10^{-13} cm, independent of the mass number, is quite reasonable from the standpoint of meson theory of nuclear forces. One would expect such a diffuse boundary potential as long as the nuclear density distribution falls off in a region smaller than the region of fall-off of the potential function. Preliminary studies[8] indicate that the composite nucleon densities calculated from this type of potential fall off more rapidly than the assumed nuclear potential.

TABLE I. Coulomb A shifts.

A	Z	ΔA_c	ΔA_a	ΔA_{net}	$v_c(r_c)$
25	12	−1.44	2.95	1.51	3.90
50	23	−4.26	9.63	5.37	6.26
75	33	−7.84	18.60	10.77	7.99
100	43	−12.18	29.83	17.65	9.56
125	53	−17.20	43.11	25.90	11.01
150	62	−22.49	57.36	34.87	12.18
175	71	−28.30	73.22	44.92	13.29
200	80	−34.61	90.59	55.98	14.36
225	89	−41.38	109.44	68.06	15.40
250	97	−48.11	128.36	80.25	16.23

The good agreement of the eigenvalues with experiment suggests that, quite apart from the fundamental significance of this phenomenological potential, this model will serve a useful role in many applications of the shell model. Good agreement is here to be interpreted in the sense of gross structure rather than fine structure, i.e., the eigenvalues of outermost particles are close from the standpoint of a range of possibilities extending from about −40 Mev to, say, +10 Mev. Since the experimental data used in the adjustment process bounds the energy region in which the shell model has been most successfully applied, one might look to the eigenvalues, and certainly to the eigenfunctions based upon this simple potential, for a realistic and quantitative realization of what has long been expected in qualitative discussions of the nuclear shell model.

The use of the critical $3s$ and $4s$ A values in the adjustment process, as well as the close resemblance between this potential and the real part of the cloudy crystal ball model potential, makes it obvious that the remarkable neutron scattering predictions of the sharp boundary cloudy crystal ball model will not be sacrificed by the substitution of the potential used here. Indeed, the scattering predictions might well be further improved by the use of a diffuse boundary potential.[9] The fact that this restricted type of nuclear potential successfully embraces both the low-energy neutron scattering problem and the bound state problem is no mean accomplishment. The widely used harmonic oscillator potential is obviously incapable of this. The square well[1] and other still more realistic potentials[10] have also been found inadequate in this regard. Other advantages of this nuclear potential are the finiteness of the potential gradient, an important consideration in correcting for the spin-orbit effect as well as other surface phenomena, and the fact that the eigenfunctions are Bessel functions, which have numerous useful

[8] K. Lee and A. E. S. Green, Phys. Rev. **99**, 1627(A) (1955).
[9] V. F. Weisskopf (private conversation).
[10] R. D. Lawson, Phys. Rev. **100**, 957(A) (1955).

analytic properties and which are among the most extensively tabulated sets of functions. The normalization constants, as well as several important diagonal matrix elements associated with this nuclear potential, have been computed and are now being prepared for publication.

ACKNOWLEDGMENTS

The writer wishes to acknowledge the helpfulness to this work of many conversations held during the Ottawa Colloquium on Theoretical Physics, particularly those with Dr. G. Breit, Dr. R. Eden, Dr. B. Jacobson, Dr. R. Jastrow, Dr. J. Levinger, and Dr. V. Weisskopf. In addition, the writer wishes to express his thanks to Dr. S. A. Moszkowski for sending him a preprint of his recent Letter, Dr. Kiuck Lee for numerous discussions, to Dr. M. A. Melvin for reading the manuscript, and to R. Berkley, J. Salacz-Dohnanyi, W. Stanley, Mrs. Rose Nelson, and Mrs. Anna Lane for for their invaluable assistance.

PHYSICAL REVIEW VOLUME 102, NUMBER 5 JUNE 1, 1956

Nuclear Magnetic Resonance Measurements of the Isotopes Barium-135 and Barium-137

H. E. WALCHLI,* *Oak Ridge National Laboratory, Oak Ridge, Tennessee*

AND

T. J. ROWLAND, *Metals Research Laboratories, Electro Metallurgical Company, Niagara Falls, New York*

(Received February 16, 1956)

By comparison with the nuclear magnetic resonance of Cl^{35}, the nuclear magnetic moments of Ba^{135} and Ba^{137} were found to be 0.832293 ± 0.000025 and 0.931074 ± 0.000055, respectively, without diamagnetic correction.

THE nuclear magnetic resonances of the barium isotopes have been determined by means of nuclear induction using a variable frequency nuclear magnetic resonance spectrometer[1] and enriched stable isotopes of barium. The electronically regulated magnet[1] having 12-inch diameter poles and a 2.13-inch gap provided a magnetic field of approximately 9200 gauss having a homogeneity of better than 0.05 gauss over the sample volume. Frequency determinations were made using a Signal Corps BC-221 frequency meter calibrated with its internal crystal and radio station WWV. The combined short-time stability of the radio-frequency oscillator and magnetic field system was greater than 1 part in 250 000.

The samples were saturated aqueous solutions of $BaCl_2$ sealed in 15-mm test tubes. No magnetic catalysts were added. Both samples exhibited signs of small $BaCl_2$ crystals in the bottom of the tube. The barium-135 sample contained 1.5 grams of barium enriched to 58.5% barium-135, and the barium-137 sample contained 1.5 grams of barium enriched to 43.5% barium-137. All frequency comparisons were made with respect to the resonance frequency of the Cl^{35} in the samples. The line widths as determined by maximum deflection of the derivative of the absorption curve was approximately 2.5 gauss. The modulating field was 1.3 gauss and it was necessary to use a relatively high level of radio-frequency field.

The results of these measurements indicate that the barium-to-chlorine frequency ratios are

$$\nu(Ba^{135})/\nu(Cl^{35})=1.01387\pm0.00002,$$

$$\nu(Ba^{137})/\nu(Cl^{35})=1.13420\pm0.00005,$$

and by calculation we find the resonance frequency ratio to be

$$\nu(Ba^{137})/\nu(Ba^{135})=1.11868\pm0.00006.$$

This result compares favorably, but is more precise than the earlier molecular beam determination by Hay[2] which gives the ratio of the barium gyromagnetic factors to be 1.1184 ± 0.0010.

Using the chlorine-to-deuterium ratio of Walchli[3] and the deuterium-to-proton ratio of Lindstrom,[4] and choosing the value of the proton moment as 2.79267 nuclear magnetons with known spins of $\frac{3}{2}$ for the barium isotopes,[5] we have calculated the nuclear moments, without diamagnetic correction, to be

$$\mu(Ba^{135})=0.832293\pm0.000025,$$

$$\mu(Ba^{137})=0.931074\pm0.000055.$$

This work was performed in the Metals Research Laboratory of the Electro Metallurgical Company, and the enriched samples were provided by the Stable Isotope Research and Production Division of the Oak Ridge National Laboratory.

* Now located at Commercial Atomic Power Activities, Westinghouse Electric Corporation, P.O. Box 355, Pittsburgh, Pennsylvania.

[1] Manufactured by Varian Associates, Palo Alto, California.

[2] R. H. Hay, Phys. Rev. **60**, 75 (1941). This report states the ratio to be 1.1174 ± 0.0010, but moment values reported give a ratio of 1.1184.

[3] H. E. Walchli, M.S. thesis, University of Tennessee, June, 1954 (unpublished); also Oak Ridge National Laboratory Report ORNL-1775 (unclassified) (unpublished).

[4] G. Lindstrom, Physica **17**, 412 (1951); Arkiv Fysik **4**, 1 (1951).

[5] J. E. Mack, Revs. Modern Phys. **22**, 64 (1950).